Exploring self-intersected N-periodics in the elliptic billiard

Ronaldo Garcia[a*], Dan Reznik[b]

[a]Fed. Univ. of Goiás, Goiânia, Brazil
ragarcia@ufg.br

[b]Data Science Consulting, Rio de Janeiro, Brazil
dreznik@gmail.com

Abstract. This is a continuation of our simulation-based investigation of N-periodic trajectories in the elliptic billiard. With a special focus on self-intersected trajectories we (i) describe new properties of $N = 4$ family, (ii) derive expressions for quantities recently shown to be conserved, and to support further experimentation, we (iii) derive explicit expressions for vertices and caustic semi-axes for several families. Finally, (iv) we include links to several animations of the phenomena.

Keywords: Invariant, elliptic, billiard, turning number, self-intersected

*AMS Subject Classification:* 51M04, 51N20, 51N35, 68T20

1. Introduction

This is a continuation of our simulation-based investigation of periodic trajectories in the elliptic billiard, i.e., Poncelet families of polygons interscribed between two confocal conics (see Appendix A for a review).

Here we focus on trajectories which are self-intersected, i.e., which wrap around the inner conic, or *caustic*, more than once (i.e., their turning number is greater than one [24]). Figure 1 (resp. 2) illustrate cases where the caustic is an ellipse (resp. hyperbola).

Specifically, we (i) describe some curious Euclidean properties, loci, and invariants of the $N = 4$ self-intersected family (Section 3); (ii) derive expressions for some conserved quantities presented in [20, 21], for both simple and self-intersected cases

---
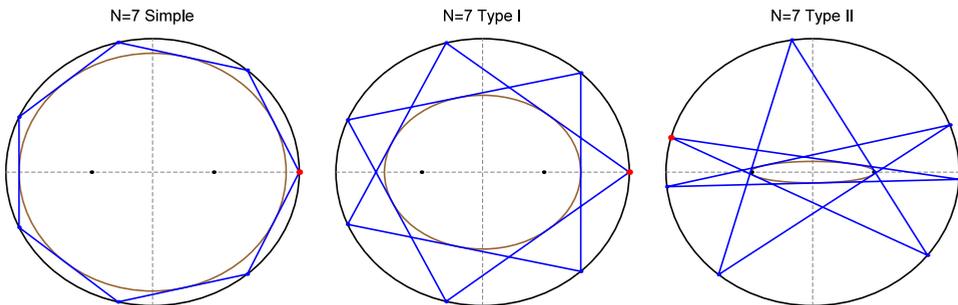
Figure 1. A simple (left), and two self-intersecting (middle, right) 7-periodics in the elliptic billiard. In the article the latter two are labeled "type I", and "type II" (turning number 2 and, 3 respectively). Video 1 Video 2

(Section 4). Interestingly, we identify a few situations where quantities conserved elsewhere become variable (reasons are unclear).

One of our goals is to encourage and support further simulation work. Toward that end, we include links to animated phenomena in the caption of most figures, all of which appear on Table 2. In Appendix B we provide expressions for both vertices and caustics for several families. Appendix C lists most symbols used herein.

1.1. Related work

Birkhoff provides a method to compute the number of possible Poncelet N-periodics, simple or not [7]. For example, for $N = 5, 6, 7, 8$ there are $1, 2, 2, 3$ distinct self-intersected closed trajectories, respectively. In [18] expressions are derived for caustic parameters which produce various types of N-periodics in the elliptic billiard. Points of self-intersections of Poncelet N-periodics are located on confocal conics of the associated Poncelet grid [16, 22, 25]. A kinematic analysis of the geometry of N=periodics using Jacobian elliptic functions is proposed in [24]. Works [13, 19] derive explicit expressions for some invariants in the $N = 3$ case (billiard triangles). Additional constructions derived from N-periodics (e.g., pedals, antipedals, etc.) are considered in [20], augmenting the list of elliptic billiard invariants to 80. In recent publications [13, 19, 21] we have described several Euclidean quantities which remain invariant over a given family, some of which have been subsequently proved [2, 5, 8].

2. Preliminaries

Throughout this article we assume the elliptic billiard is the ellipse:

$$f(x, y) = \left(\frac{x}{a}\right)^2 + \left(\frac{y}{b}\right)^2 = 1, \quad a > b > 0.$$

Below we refer to trajectories with turning number 1, 2, 3, and 4, by simple, type I, type II, and type III, respectively.

2.1. A word about our proof method

We omit most proofs as they have been produced by a consistent process, namely: (i) using the expressions in Appendix B, find the vertices an axis-symmetric N-periodic, i.e., whose first vertex $P_1 = (a, 0)$; (ii) obtain a symbolic expression for the invariant of interest; (iii) derive an expression for the given quantity for a generic trajectory parametrized by t; (iv) using CAS simplification, show that t can be eliminated, i.e., that (iii) reduces to (ii).

3. Properties of self-intersected 4-periodics

The family of simple 4-periodics in the elliptic billiard are parallelograms [9]. In this section consider self-intersected 4-periodics whose caustic is a confocal hyperbola; see Figure 2. We start deriving simple facts about them and then proceed to certain elegant properties.

Proposition 3.1. *The perimeter L of the self-intersected 4-periodic is given by:*

$$L = \frac{4a^2}{c}, \quad with \quad c^2 = a^2 - b^2. \tag{3.1}$$

Proof. Since perimeter is constant, use as the $N = 4$ candidate the centrally-symmetric one, Figure 2 (right). Its upper-right vertex $P_1 = (x_1, y_1)$ is such that it reflects a vertical ray toward $-P_1$, and this yields:

$$P_1 = (x_1, y_1) = \left[\frac{a\sqrt{a^2 - 2b^2}}{bc}, \frac{b}{c} \right].$$

Since $P_2 = -P_1$ its perimeter is $L = 2(|2P1| + 2y_1)$ and this can be simplified to (3.1), invariant over the family. $\square$

with $a/b \geq \sqrt{2}$. At $a/b = \sqrt{2}$ the family is a straight line from top to bottom vertex of the elliptic billiard, Figure 2 (left).

Observation 3.2. *At $a/b = \sqrt{1 + \sqrt{2}} \simeq 1.55377$ the two self-intersecting segments of the bowtie do so at right-angles.*

Observation 3.3. *At $a/b \simeq 1.55529$ the perimeter of the bowtie equal that of the elliptic billiard.*

Referring to Figure 3:

Proposition 3.4. *The $N = 4$ self-intersected family has zero signed orbit area and zero sum of signed cosines, i.e., both are invariant. The same two facts are true for its outer polygon. Furthermore the latter has zero sum of double-angle signed cosines.*
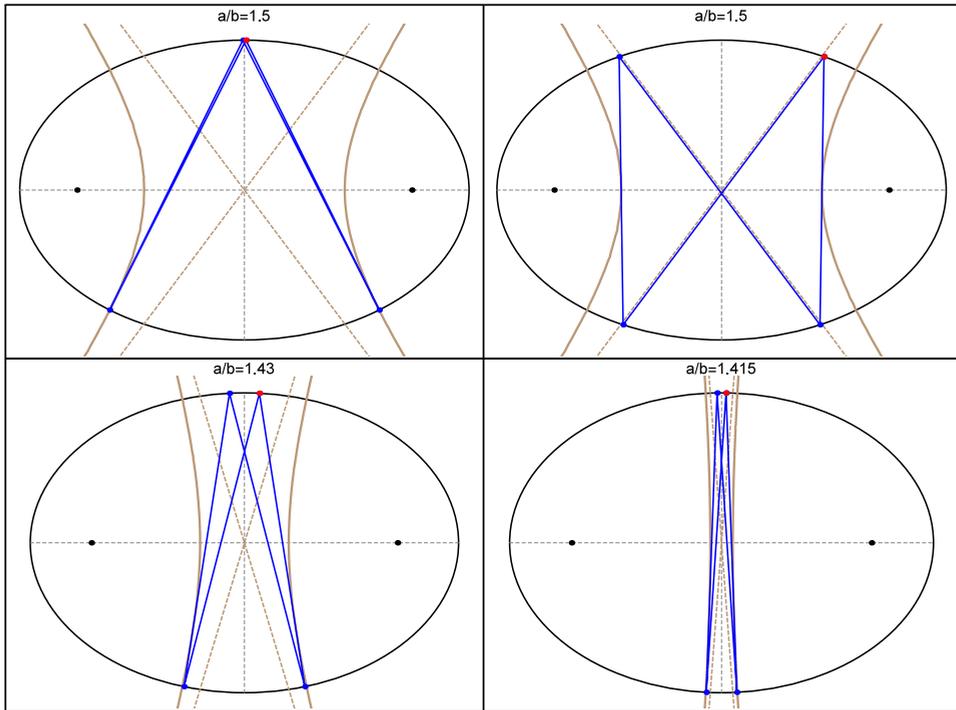
Figure 2. In the top left (resp. top right) an $N = 4$ self-intersected trajectory is shown near its "doubled up" (resp. almost symmetric) position. In both cases trajectory segments are tangent to a hyperbolic caustic (brown). As the aspect ratio of the elliptic billiard decreases (bottom left and right), the family is squeezed into an ever narrower space between the approaching branches of the caustic. Video

Proof. This stems from the fact all self-intersected 4-periodics are symmetric with respect to the elliptic billiard's minor axis. ∎

Referring to Figure 3, as in Appendix B.2, let vertex P_1 of the self-intersected 4-periodic be parametrized as $P_1(u) = \left[au, b\sqrt{1 - u^2}\right]$, with $|u| \leq \frac{a}{c^2}\sqrt{a^2 - 2b^2}$. Then:

Theorem 3.5. *The four vertices of the self-intersected 4-periodic (resp. outer polygon) are concyclic with the two foci of the elliptic billiard, on a circle $\mathcal{C}$ of variable radius R (resp. R') whose center C (resp. C') lies on the y axis. These are given by:*

$$C = \left[0, \frac{c^2u^2 - a^2 + 2b^2}{2b\sqrt{1 - u^2}}\right], \qquad C' = \left[0, -\frac{2bc^2\sqrt{1 - u^2}}{a^2 + (u^2 - 2)c^2}\right],$$
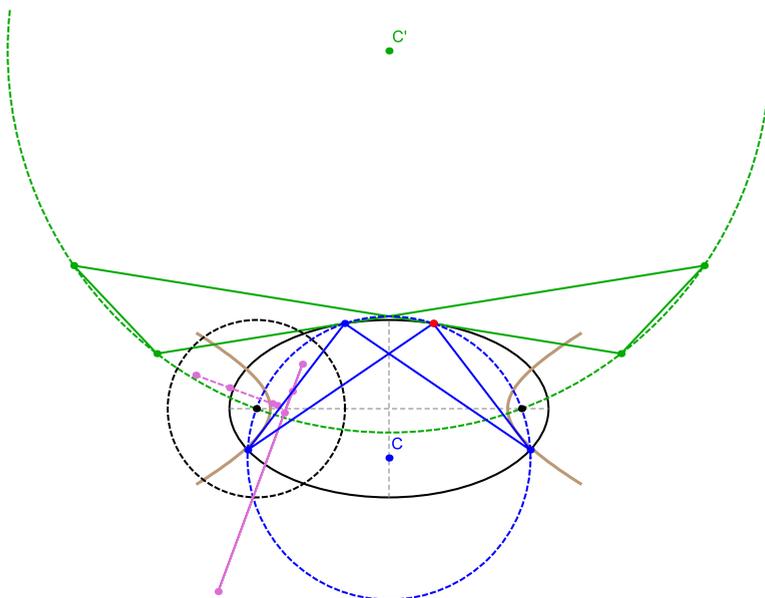
Figure 3. The vertices of the self-intersected 4-periodic (blue) are concyclic with the foci of the elliptic billiard on a circle (dashed blue) centered on C. The inversive polygon (pink segment) with respect to a unit circle $C^\dagger$ (dashed black) centered on the left focus degenerates to a segment along the radical axis of the two circles. The vertices of the outer polygon (green) are also concyclic with the foci on a distinct circle (dashed green) centered on C'. Therefore the outer's inversive polygon (dotted pink) is also a segment along the radical axis of this circle with $C^\dagger$. Note the two radical axes are dynamically perpendicular. Video 1 Video 2

$$R = \frac{a^2 - c^2 u^2}{2b\sqrt{1 - u^2}}, \qquad\qquad R' = \frac{c(c^2 u^2 - a^2)}{a^2 + (u^2 - 2)c^2}.$$

Corollary 3.6. *The half harmonic mean of R^2 and R'^2 is invariant and equal to $c^2 = a^2 - b^2$, i.e., $1/R^2 + 1/R'^2 = 1/c^2$.*

Note: the above Pythagorean relation implies that the polygon whose vertices are a focus, and the inversion of C, C', O (center of the elliptic billiard) with respect to a unit circle centered on said focus, is a rectangle of sides $1/R$ and $1/R'$ and diagonal $1/c$.

Remarkably:

Corollary 3.7. *Over the self-intersected $N = 4$ family, the power of the origin with respect to both $\mathcal{C}$ and $\mathcal{C}'$ is invariant and equal to $b^2 - a^2$.*

Referring to Figure 4, $N = 4$ self-intersected trajectories are *anti-parallelograms* [27]: these are images of vertices of a parallelogram reflected on opposite diagonals.

A well-know property is that the midpoints of its four segments are collinear on a horizontal line parallel to a diagonal.

Observation 3.8. *The locus of midpoints of $N = 4$ self-intersected segments is an ∞-shaped quartic curve given by:*

$$c^2(b^2x^2 + a^2y^2)^2 - b^4a^2\big((a^2 - 2b^2)x^2 - a^2y^2\big) = 0.$$

Furthermore, the above quartic is tangent to the confocal hyperbolic caustic at its vertices $[\pm a\sqrt{a^2 - 2b^2}/c, 0]$.
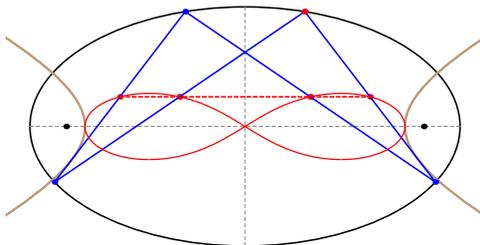
Figure 4. The midpoints of each of the four segments of self-intersected 4-periodics are collinear on a horizontal line. Their locus is an ∞-shaped quartic which touches the caustic at its vertices.
Video

Let $\mathcal{P}^\dagger$ (resp. $\mathcal{Q}^\dagger$) denote the inversive polygon of 4-periodics (resp. its outer polygon) wrt a unit circle $\mathcal{C}^\dagger$ centered on one focus. From properties of inversion:

Corollary 3.9. $\mathcal{P}^\dagger$ *(resp. $\mathcal{Q}^\dagger$) has four collinear vertices, i.e., it degenerates to a segment along the radical axis of $\mathcal{C}^\dagger$ and $\mathcal{C}$ (resp. $\mathcal{C}'$).*

Proposition 3.10. *The two said radical axes are perpendicular.*

Proof. It is enough to check that the vectors $C - [-c, 0]$ and $C' - [-c, 0]$ are orthogonal. Observe that when $u^2 = (a^2 - 2b^2)/c = (2c^2 - a^2)/c$ the outer polygon is contained in the horizontal axis. $\square$

Observation 3.11. *The pairs of opposite sides of the outer polygon to self-intersected 4-periodics intersect at the top and bottom of the circle (C, R) on which the 4-periodic vertices are concyclic.*

4. Deriving both simple and self-intersected invariants

In this section, we derive expressions for selected invariants introduced in [20], specifically for "low-N" cases, e.g., $N = 3, 4, 5, 6, 8$. In that publication, each

invariant is identified by a 3-digit code, e.g., k_{101}, k_{102}, etc. Table 1 lists the invariants considered herein. The quantities involved are defined next.

Table 1. List of selected invariants taken from [20] as well as the low-N cases (column "derived") for expressions are derived herein, where N refers to simple N-periodics, and N_i (resp. N_{ii}) refers to type I (resp. type II) N-periodics. Refer to Table 3 for the meaning of symbols in column "invariant". † L_1 was co-discovered with P. Roitman. A closed-form expression for k_{119} was derived by H. Stachel; see (A.1).

| code	invariant	valid N	derived	proofs
k_{101}	$\sum \cos\theta_i$	all	$JL-N$	[2, 5]
k_{102}	$\prod \cos\theta_i'$	all	$3,4,5,5_i,6,6_i,6_{ii}$	[2, 5]
k_{103}	A'/A	odd	$3,5,5_i$	[2, 8]
k_{104}	$\sum \cos(2\theta_i')$	all	$3,4,4_i,5,5_i,6,6_i,8$	[1]
k_{105}	$\prod \sin(\theta_i/2)$	odd	$3,5,5_i$	[1]
k_{106}	$A'A$	even	$4,4_i,6,6_i,6_{ii}$	[8]
k_{110}	$A\,A''$	even	$4,4_i,6,6_i,6_{ii}$	?
$^\dagger k_{119}$	$\sum \kappa_i^{2/3}$	all	$3,4,6$	[2, 23]
$k_{802,a}$	$\sum 1/d_{1,i}$	all	$3,4,6$	[2]
k_{803}	$L_1^\dagger$	all	$3,4,6$	?
$^\dagger k_{804}$	$\sum \cos\theta_{1,i}^\dagger$	$\neq 4$	3	?
$k_{805,a}$	$A\,A_1^\dagger$	$\equiv 0 \pmod 4$	$4,4_i,8$	?
k_{806}	$A/A_1^\dagger$	$\equiv 2 \pmod 4$	6	?
k_{807}	$A_1^\dagger . A_2^\dagger$	odd	3	?

Let θ_i denote the ith N-periodic angle. Let A the signed area of an N-periodic. Referring to Figure 5, singly-primed quantities (e.g., θ_i', A', etc.), etc., always refer to the *outer polygon*: its sides are tangent to the elliptic billiard at the P_i. Likewise, doubly-primed quantities (θ_i'', A'', etc.) refer to the *inner polygon*: its vertices lie at the touchpoints of N-periodic sides with the caustic. More details on said quantities appear in Appendix A.

Recall $k_{101} = JL - N$, as introduced in [5, 19].

Referring to Figure 6, the f_1-*inversive polygon* has vertices at inversions of the P_i with respect to a unit circle centered on f_1. Quantities such as $L_1^\dagger$, $A_1^\dagger$, etc., refer to perimeter, area, etc. of said polygon.
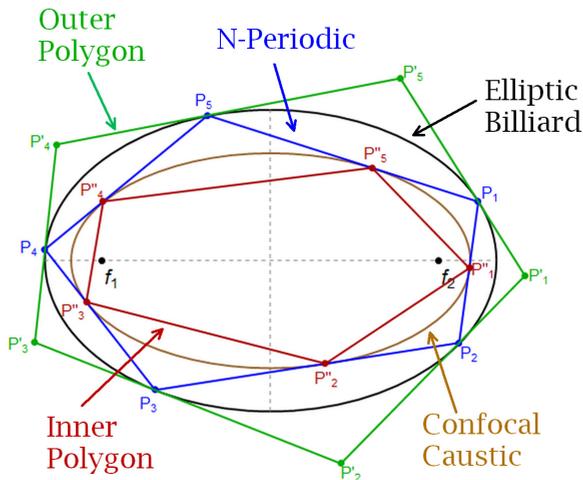
Figure 5. The *N*-periodic (blue), is associated with an outer (green) and an inner (red) polygons. The former's sides are tangent to the billiard (black) at each *N*-periodic vertex; the latter's vertices are the tangency points of *N*-periodics sides to the confocal caustic (brown). Video
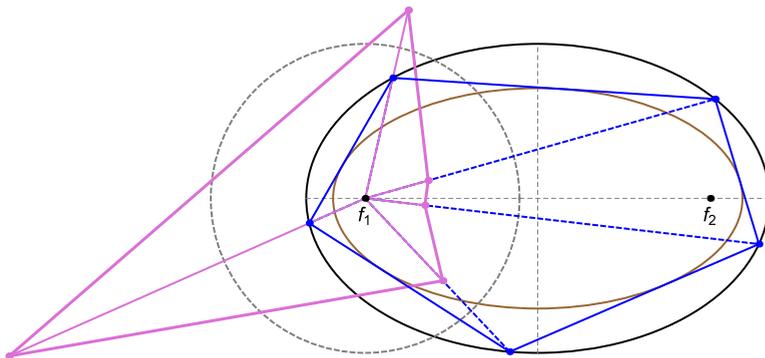
Figure 6. Focus-inversive 5-periodic (pink) whose vertices are inversions of the P_i (blue) with respect to a unit circle (dashed black) centered on f_1. It turns out its perimeter is also invariant over the family as is the sum of its spoke lengths (pink lines). Video

4.1. Invariants for $N = 3$

As before, let $\delta = \sqrt{a^4 - a^2 b^2 + b^4}$. For $N = 3$ explicit expressions for J and L have been derived [13]:

$$J = \frac{\sqrt{2\delta - a^2 - b^2}}{c^2}, \quad L = 2(\delta + a^2 + b^2)J. \tag{4.1}$$

When $a = b$, $J = \sqrt{3}/2$ and when $a/b \to \infty$, $J \to 0$.

Proposition 4.1. *For $N = 3$, $k_{102} = (JL)/4 - 1$.*

Proof. We've shown $\sum_{i=1}^{3} \cos \theta_i = JL - 3$ is invariant for the $N = 3$ family [13]. For any triangle $\sum_{i=1}^{3} \cos \theta_i = 1 + r/R$ [28], so it follows that $r/R = JL - 4$ is also invariant. Let r_h, R_h be the Orthic Triangle's Inradius and Circumradius. The relation $r_h/R_h = 4 \prod_{i=1}^{3} |\cos \theta_i|$ is well-known [28, Orthic Triangle]. Since a triangle is the Orthic of its Excentral Triangle, we can write $r/R = 4 \prod_{i=1}^{3} \cos \theta_i'$, where θ_i' are the Excentral angles which are always acute [28] (absolute value can be dropped), yielding the claim. □

Proposition 4.2. *For $N = 3$, $k_{103} = k_{109} = 2/(k_{101} - 1) = 2/(JL - 4)$.*

Proof. Given a triangle A' (resp. A'') refers to the area of the Excentral (resp. Extouch) triangles. The ratios A'/A and A/A'' are equal. Actually, $A'/A = A/A'' = (s_1 s_2 s_3)/(r^2 L)$, where s_i are the sides, L the perimeter, and r the Inradius [28, Excentral, Extouch]. Also known is that $A'/A = 2R/r$ [14]. Since $r/R = \sum_{i=1}^{3} \cos \theta_i - 1 = k_{101} - 1$ [28, Inradius], the result follows. □

Proposition 4.3. *For $N = 3$, $k_{104} = -k_{101}$ and is given by:*

$$k_{104} = \frac{(a^2 + b^2)(a^2 + b^2 - 2\delta)}{c^4} = 3 - JL.$$

Proposition 4.4. *For $N = 3$, $k_{105} = (JL)/4 - 1 = k_{102}$.*

Proof. Let r, R be a triangle's Inradius and Circumradius. The identity $r/R = 4 \prod_{i=1}^{3} \sin(\theta_i/2)$ holds for any triangle [28, Inradius], which with Proposition 4.1 This completes the proof. □

Proposition 4.5. *For $N = 3$, k_{119} is given by:*

$$(k_{119})^3 = \frac{2J^3 L}{(JL - 4)^2}, \quad k_{119} = \frac{a^2 + b^2 + \delta}{(ab)^{\frac{4}{3}}}.$$

Proof. Use the expressions for L, J in (4.1). □

Proposition 4.6. *For $N = 3$:*

$$k_{802,a} = \frac{a^2 + b^2 + \delta}{ab^2} = \frac{J\sqrt{2}\sqrt{JL + \sqrt{9 - 2JL} - 3}}{JL - 4},$$

$$k_{803} = \rho \frac{\sqrt{(8a^4 + 4a^2 b^2 + 2b^4)\delta + 8a^6 + 3a^2 b^4 + 2b^6}}{a^2 b^2},$$

$$k_{804} = \frac{\delta(a^2 + c^2 - \delta)}{a^2 c^2},$$

$$k_{807} = \frac{\rho^8}{8a^8 b^2} \left[(a^4 + 2a^2 b^2 + 4b^4)\delta + a^6 + (3/2)a^4 b^2 + 4b^6 \right].$$

Note: ρ is the radius of the inversion circle, included above for unit consistency. By default $\rho = 1$.

4.2. Invariants for $N = 4$

Proposition 4.7. *For simple $N = 4$, $k_{102} = 0$.*

Proof. Simple 4-periodics are parallelograms [9] whose outer polygon is a rectangle inscribed in Monge's Orthoptic Circle [19]. This finishes the proof. □

Proposition 4.8. *For simple $N = 4$, $k_{104} = -4$.*

Proof. As in Proposition 4.7, outer polygon is a rectangle. □

Let $\kappa_a = (ab)^{-2/3}$ denote the affine curvature of the ellipse and $r_m = \sqrt{a^2 + b^2}$ the radius of Monge's orthoptic circle [28].

Proposition 4.9. *For simple $N = 4$:*

$$k_{106} = 8a^2b^2, \qquad\qquad k_{110} = \frac{2a^4b^4}{(a^2+b^2)^2},$$

$$k_{119} = \frac{2(a^2+b^2)}{(ab)^{\frac{4}{3}}} = 2(\kappa_a r_m)^2, \qquad k_{802,a} = \frac{2(a^2+b^2)}{ab^2},$$

$$k_{803} = \frac{4\rho^2\sqrt{a^2+b^2}}{b^2}, \qquad\qquad k_{805,a} = 4.$$

Note: when $b = 1$, k_{803} is equal to the perimeter of the 4-periodic; see (B.1).

Counter-example 4.10. *Experimentally, k_{804} is invariant for all simple N-periodics, except when $N = 4$.*

Restating results from Proposition 3.4:

Observation 4.11. *Over self-intersected $N = 4$, $k_{101} = k_{104} = 0$. Since A is null, so are k_{106}, k_{110}, and $k_{805,a}$.*

We leave as exercises the derivation of expressions for k_{102}, k_{119}, $k_{802,a}$, and k_{803} over self-intersected $N = 4$.

4.3. Invariants for $N = 5$

As seen in Appendix B, the vertices of 5-periodics can only be obtained via an implicitly-defined caustic. Namely, we first numerically obtain the caustic semi-axes and then compute a axis-symmetric polygon tangent to it. Note that both simple and self-intersected 5-periodics possess an elliptic confocal caustic; see Figure 7.

Proposition 4.12. *For simple (resp. self-intersected) $N = 5$, k_{102} is given by the largest negative (resp. positive) real root of the following 6th-degree polynomial:*

$$k_{102} : 1024c^{20}x^6 + 2048(a^4 + a^3b - ab^3 + b^4)(a^4 - a^3b + ab^3 + b^4)c^{12}x^5$$
$$+ 256(4a^{12} - a^{10}b^2 + 32a^8b^4 - 22a^6b^6 + 32a^4b^8 - a^2b^{10} + 4b^{12})c^8x^4$$

$$- 64a^2b^2(4a^{12} - 27a^{10}b^2 + 38a^8b^4 - 126a^6b^6 + 38a^4b^8 - 27a^2b^{10} + 4b^{12})c^4x^3$$
$$- 16a^6b^6(7a^8 - 96a^6b^2 + 114a^4b^4 - 96a^2b^6 + 7b^8)x^2$$
$$- 8a^8b^8(7a^4 + 30a^2b^2 + 7b^4)x - a^{10}b^{10} = 0.$$
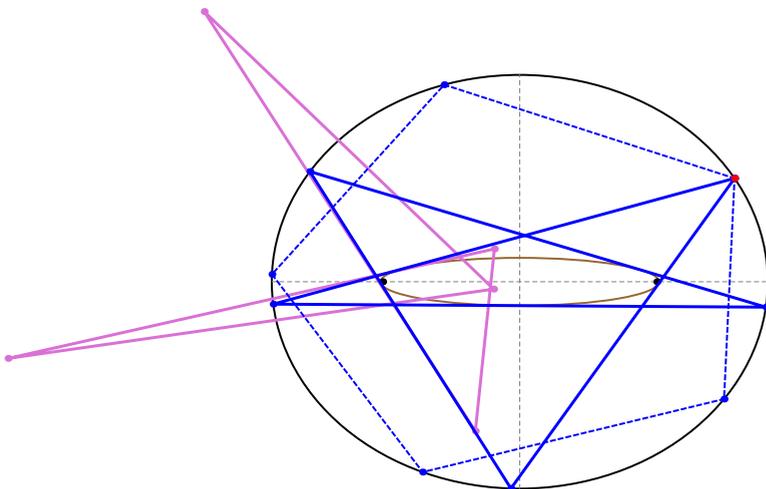
Figure 7. A simple (blue) and self-intersected (dashed blue) 5-periodic, as well as the former's focus-inversive polygon (pink).
Video

Proposition 4.13. *For simple (resp. self-intersected) $N = 5$, k_{103} is given by the smallest (resp. largest) real root greater than 1 of the following 6th-degree polynomial:*

$$k_{103} : a^6b^6x^6 - 2b^2a^2\left(4a^8 - a^6b^2 - a^2b^6 + 4b^8\right)x^5$$
$$- b^2a^2\left(4a^8 + 19a^6b^2 - 62a^4b^4 + 19a^2b^6 + 4b^8\right)x^4$$
$$+ 12b^2a^2\left(a^4 + b^4\right)c^4x^3 + \left(4a^8 + 19a^6b^2 + 66a^4b^4 + 19a^2b^6 + 4b^8\right)c^4x^2$$
$$+ \left(2a^8 + 12a^6b^2 + 36a^4b^4 + 12a^2b^6 + 2b^8\right)c^4x - c^{12}.$$

Proposition 4.14. *For simple (resp. self-intersected) $N = 5$, k_{104} is given by the only negative (resp. smallest largest) real root of the following 6th-degree polynomial:*

$$c^{12}x^6 - 2(a^4 + 10a^2b^2 + b^4)c^8x^5 - (37a^4 - 6a^2b^2 + 37b^4)c^8x^4$$
$$+ 4(5a^8 + 92a^6b^2 + 62a^4b^4 + 92a^2b^6 + 5b^8)c^4x^3$$
$$+ (423a^{12} - 354a^{10}b^2 + 2713a^8b^4 - 4796a^6b^6 + 2713a^4b^8 - 354a^2b^{10} + 423b^{12})x^2$$
$$+ (270a^{12} + 740a^{10}b^2 - 3630a^8b^4 + 7160a^6b^6 - 3630a^4b^8 + 740a^2b^{10} + 270b^{12})x$$
$$- 675a^{12} - 850a^{10}b^2 + 1075a^8b^4 - 3900a^6b^6 + 1075a^4b^8 - 850a^2b^{10} - 675b^{12}.$$

Proposition 4.15. *For simple (resp. self-intersected) $N = 5$, k_{105} is given by the largest positive real root (resp. the symmetric value of the largest negative root) of the following 6th-degree polynomial:*

$$2^{10}c^{20}x^6 + 2^{10}(2a^{12} + a^{10}b^2 + 26a^8b^4 + 70a^6b^6 + 26a^4b^8 + a^2b^{10} + 2b^{12})c^8x^5$$
$$+ 2^8(4a^{12} + 30a^{10}b^2 + 71a^8b^4 + 350a^6b^6 + 71a^4b^8 + 30a^2b^{10} + 4b^{12})c^8x^4$$
$$+ 2^6a^2b^2(4a^{12} + 9a^{10}b^2 - 318a^8b^4 - 126a^6b^6 - 318a^4b^8 + 9a^2b^{10} + 4b^{12})c^4x^3$$
$$- 2^6a^2b^2(8a^{16} - 53a^{14}b^2 + 253a^{12}b^4 - 1041a^{10}b^6 + 1650a^8b^8$$
$$- 1041a^6b^{10} + 253a^4b^{12} - 53a^2b^{14} + 8b^{16})x^2$$
$$- 2^4a^2b^2(16a^{16} - 12a^{14}b^2 + 5a^{12}b^4 + a^{10}b^6 + 2a^8b^8 + a^6b^{10}$$
$$+ 5a^4b^{12} - 12a^2b^{14} + 16b^{16})x$$
$$- a^{10}b^{10}.$$

4.4. Invariants for $N = 6$

Referring to Figure 5 (right):

Proposition 4.16. *For simple $N = 6$:*

$$k_{102} = a^2b^2/(4(a+b)^4) = (JL - 4)^2/64,$$
$$k_{104} = k_{101} = JL - 6,$$
$$k_{106} = \frac{4b^2(2a+b)a^2(a+2b)}{(a+b)^2} = -\frac{(JL-12)(JL-4)^2}{16J^4},$$
$$k_{110} = \frac{4a^3b^3(2a+b)^2(a+2b)^2}{(a+b)^6} = -\frac{(JL-12)^2(JL-4)^3}{256J^4},$$
$$k_{119}^3 = \frac{2^5J^5L^3}{(JL-4)^4},$$
$$k_{802,a} = \frac{2(a^2+ab+b^2)}{ab^2} = \frac{4J^2L(1+\sqrt{JL-3})}{(JL-4)^2},$$
$$k_{803} = 2\rho^2(2a^2+2ab-b^2)/(ab^2),$$
$$k_{806} = 4\rho^{-4}a^3b^4/((2a-b)(a+b)^2).$$

4.5. $N = 6$ self-intersecting

Only two $N = 6$ topologies can produce closed trajectories, both with two self-intersections. These will be referred to as type I and type II, and are depicted in Figures 8, and 9, respectively.
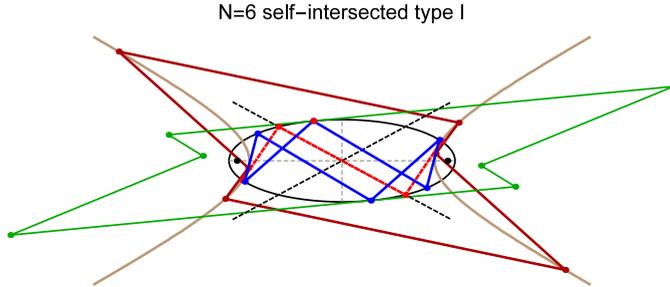
Proposition 4.17. *For $N = 6$ type I:*

$$k_{102} = a^2b^2/(4(a-b)^4) = (J\,L - 4)^2/64,$$

$$k_{104} = -\frac{2(a^2 - 4ab + b^2)}{(a - b)^2} = JL - 6 = k_{101},$$

$$k_{106} = 4a^2b^2(a - 2b)(2a - b)/(a - b)^2 = -(JL - 12)(JL - 4)^2/(16J^4),$$

$$k_{110} = \frac{-4a^3b^3(a - 2b)^2(2a - b)^2}{(a - b)^6} = \frac{(JL - 12)^2(JL - 4)^3}{2^8J^4}.$$

N=6 self−intersected type I

Figure 8. Type I self-intersected 6-periodic (blue) and its doubled-up configuration (dashed red), both tangent to a hyperbolic confocal caustic (brown). Its asymptotes (dashed black) pass through the center of the elliptic billiard. Also shown are the outer (green) and inner (dark red) polygons. Video

N=6 self−intersected type II
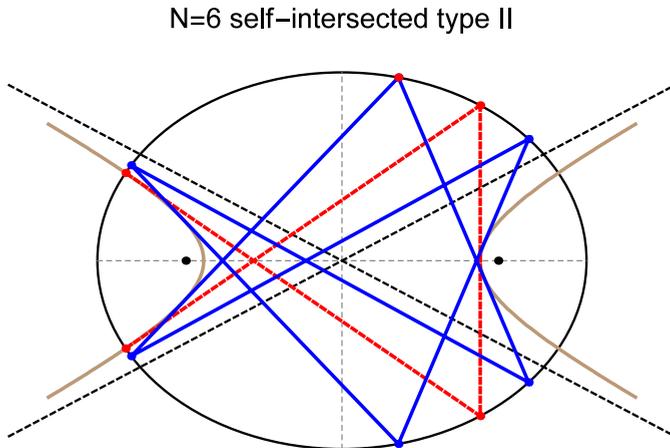
Figure 9. Self-intersected 6-periodic (type II) shown both at one of its doubled-up configurations (dashed red) and in general position (blue). Segments are tangnet to a hyperbolic confocal caustic (brown) whose asymptotes (dashed black) pass through the center of the elliptic billiard. Also shown is the outer polygon (green) which in this case is always simple. Video

Proposition 4.18. *For $N = 6$ type II:*

$k_{102} = a^2(a-c)^2/(4c^4) = (JL-8)^2(JL-4)^2/1024,$

$$k_{104} = \frac{2(a^2 - ac + c^2)(a^2 - ac - c^2)}{c^4} = \frac{(J^2L^2 - 12JL + 16)(J^2L^2 - 12JL + 48)}{128},$$
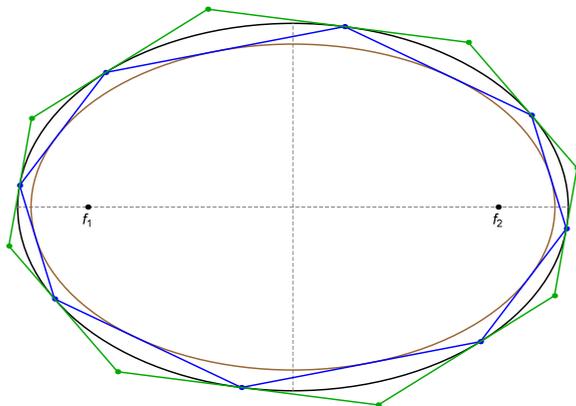
$k_{106} = k_{110} = 0.$

Note (i) in contrast with the above, $k_{104} = k_{101} = JL - 6$ for both $N = 6$ simple and type I, and (ii) k_{106} and k_{110} are nil since both A and A' vanish.

Counter-example 4.19. *Experimentally, k_{804} is invariant for $N = 6$ simple, and type I. However, it is variable for $N = 6$ type II.*

4.6. Invariants for $N = 8$

Referring to Figure 10:

Figure 10. The outer polygon (green) to a simple 8-periodic has null sum of double cosines. Video

Proposition 4.20. *For simple $N = 8$, k_{102} is given by $(1/2^{12})(JL-4)^2(JL-12)^2$.*

Proposition 4.21. *For $N = 8$, $k_{104} = 0$.*

Proof. Using the CAS, we checked that k_{104} vanishes for an 8-periodic in the "horizontal" position, i.e., $P_1 = (a, 0)$. Since k_{104} is invariant [2], this completes the proof. □
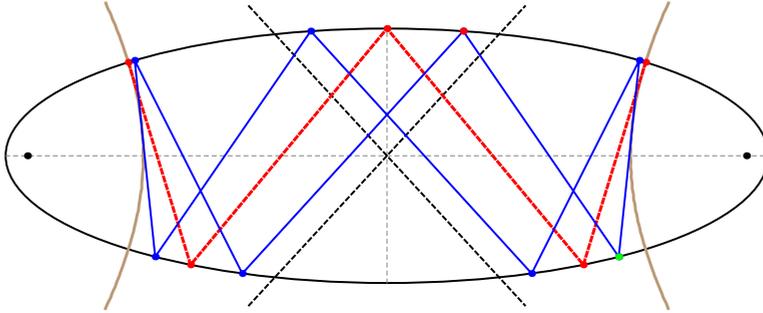
4.7. $N = 8$ self-intersected

There are 3 types of self-intersected 8-periodics [6], here called type I, II, and III. These correspond to trajectories with turning numbers of 0, 2, and 3, respectively. These are depicted in Figures 11, 12, and 13.

Observation 4.22. *The signed area of $N = 8$ type I is zero.*

Referring to Figure 13, the following is related to the Poncelet Grid [16] and the Hexagramma Mysticum [3]:

Observation 4.23. *The outer polygon to $N = 8$ type III is inscribed in an ellipse.*

Figure 11. Self-intersecting 8-periodic of type I (blue) and its doubled-up configuration (dashed red) in $a/b = 3$ ellipse. Trajectory segments are tangent to a confocal hyperbolic caustic (brown). Video
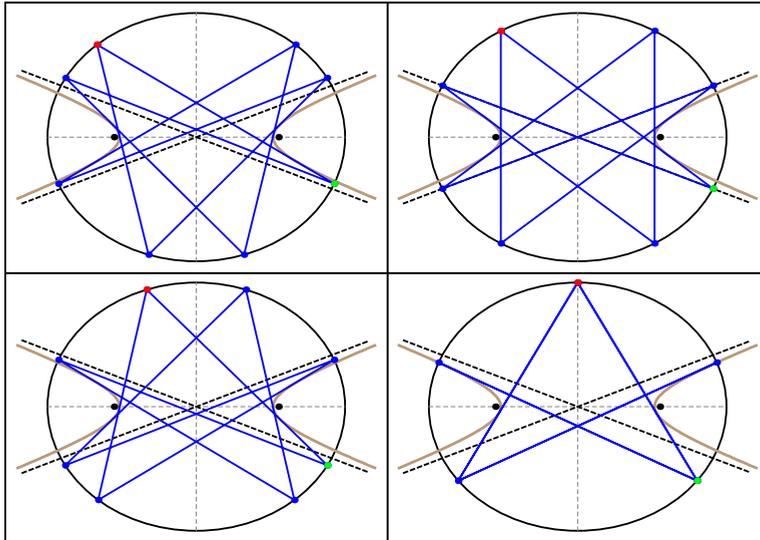
Figure 12. Four positions of a type-II self-intersecting 8-periodic trajectory (blue) in an $a/b = 1.2$ elliptic billiard, at four different locations of a starting vertex (red). In general position, these have turning number 2. Also shown is confocal hyperbolic caustic (brown). Video
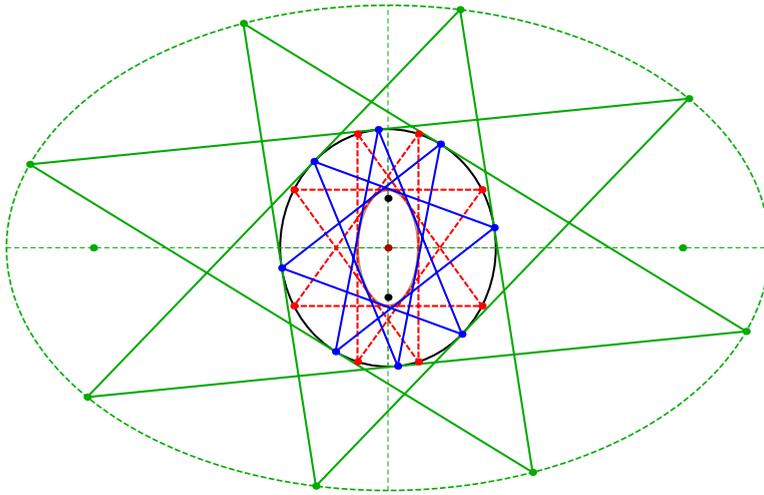
Figure 13. A type-III self-intersected 8-periodic trajectory (blue) and its doubled-up configuration (dashed red) in an $a/b = 1.1$ elliptic billiard (shown rotated by $90°$ to save space). The turning number is 3. The confocal caustic is an ellipse (brown). Also shown is the outer polygon (green) whose vertices are inscribed in an axis-aligned, concentric ellipse (dashed green), a result related to [3].
Video

5. When invariants are variable

The sum of focus-inversive cosines (k_{804}) is invariant in all N-periodics so far studied, excepting $N = 4$ simple and $N = 6$ type II; see Counter-examples 4.10 and 4.19. Notice that for the former the area of simple 4-periodics is non-zero while the sum of cosines vanishes; in the latter case the situation reverses: the area of type II 6-periodics vanishes and the sum of cosines is non-zero. Could either vanishing quantity be the reason k_{804} becomes variable, e.g., is this introducing a pole in the meromorphic functions on the elliptic curve assumed in the proof of invariants in [2]?

6. Videos

Animations illustrating some of the above phenomena are listed on Table 2.

Acknowledgments

The authors are grateful for the constructive comments by the referee. We would also like to thank Arseniy Akopyan, Jair Koiller, Pedro Roitman, Richard Schwartz,

Table 2. Videos illustrating some phenomena. The last column is
clickable and/or provides the YouTube code.

id	Title	youtu.be/<...>
01	$N = 3-6$ orbits and caustics	Y3q35DObfZU
02	$N = 5$ with inner and outer polygons	PRkhrUNTXd8
03	$N = 6$ zero-area antipedal @ $a/b = 2$	HMhZW_kWLGw
04	$N = 8$ outer poly's null sum of double cosines	GEmV_U4eRIE
05	$N = 4$ self-int. and its outer polygon	C8W2e6ftfOw
06	$N = 4$ self-int. vertices concyclic w/ foci	207Ta31Pl9I
07	$N = 4$ self-int. vertices and outer concyclic w/ foci	4g-JBshX10U
08	$N = 4$ self-int. coll. segment midpts. & 8-shaped locus	GZCrek7RTpQ
09	$N = 5$ self-int. (pentagram)	ECe4DptduJY
10	$N = 6$ self-int. type I	fOD85MNrmdQ
11	$N = 6$ self-int. type II	gQ-FbSq7wWY
12	$N = 7$ self-int. type I and II	yzBG8rgPUP4
13	$N = 8$ self-int. type I	5Lt9atsZhRs
14	$N = 8$ self-int. type II	3xpGnDxyi0
15	$N = 8$ self-int. type III	JwD_w5ecPYs
16	$N = 3$ inversives rigidly-moving circumbilliard	LOJK5izTctI
17	$N = 3$ inversive: invariant area product	OL2uMk2xyKk
18	$N = 5$ inversives: invariant area product	bTkbdEPNUOY
19	$N = 5$ self-int. inversive: invariant perimenter	LuLtbwkfSbc
20	$N = 5$ and outer inversives: invariant area ratio	eG4UCgMkKl8
21	$N = 7$ self-int. type I inversives: invariant area product	BRQ39O9ogNE

A. Review: Elliptic billiard

In *mathematical billiards* one studies the constant-velocity motion of a point mass as it undergoes elastic collisions with a chosen boundary (smooth or polygonal). A special case is when the boundary is an ellipse, called the *elliptic billiard*. Since consecutive trajectory segments are bisected by the ellipse normal, Graves' theorem implies these will be tangent to a confocal caustic [26]. Equivalently, a certain quantity, known as Joachimsthal's constant J, is conserved [4, 10]. Uniquely amongst all planar billiards, the elliptic billiard is an *integrable* dynamical system, i.e., its phase-space if foliated by tori or equivalently, the billiard-map is volume preserving [15].

Referring to Figure 14, for an arbitrary starting condition of a point mass, its trajectory is in general aperiodic (i.e., space filling). But if certain conditions are

met, known as *Cayley conditions* [11], a trajectory can be made to close after N reflections or "bounces"; see Figure 15.

The elliptic billiard can be regarded as a special case of Poncelet's porism: if an N-gon can be found inscribed in a first conic $\mathcal{C}$ and circumscribing a second one $\mathcal{C}'$, a 1d family of such N-gons exists with a vertex at an arbitrary point on $\mathcal{C}$.

Therefore, if in the elliptic billiard a certain trajectory is found to close within N segments, a family of such trajectories exists. Remarkably, over such a family, perimeter L is conserved [26].
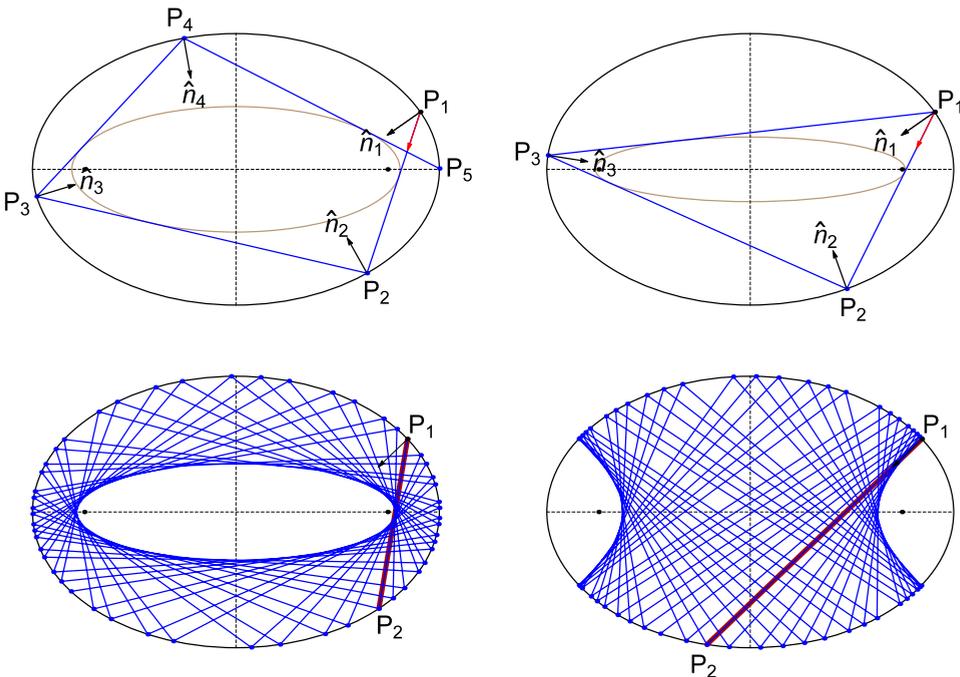
Figure 14. Top left: first four segments of a trajectory in an elliptic billiard. Each bounce is elastic (consecutive segments $P_i P_{i+1}$ are bisected by ellipse normals $\hat{n}_i$). All segments are tangent to a confocal caustic (brown). **Top right**: A trajectory which closes in 3 iterations (it is 3-periodic). **Bottom left**: An aperiodic trajectory such that a first segment $P_1 P_2$ does not pass between the foci; all subsequent segments won't either, and the caustic is an ellipse. **Bottom right**: $P_1 P_2$ now passes between the foci; all subsequent segments will as well, and all will be tangent to hyperbolic caustic.

Joachimsthal's constant is equivalent to stating that every trajectory segment is tangent to a confocal caustic [26]. Equivalently, a positive quantity J remains invariant at every

$$J = \frac{1}{2} \nabla f_i . \hat{v} = \frac{1}{2} |\nabla f_i| \cos \alpha,$$
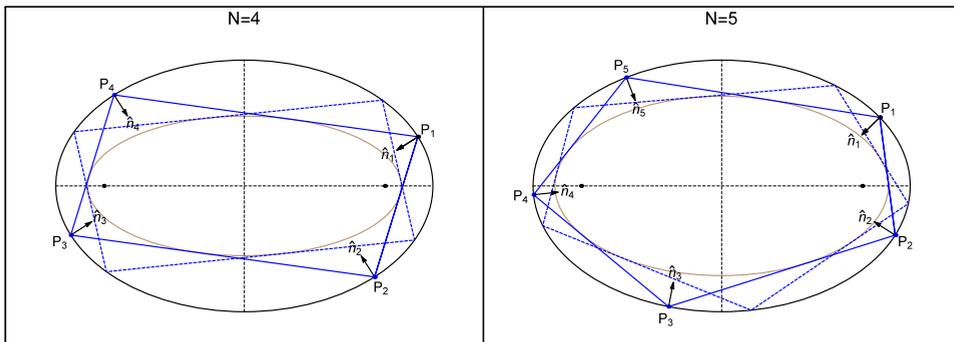
Figure 15. Elliptic Billiard (black) 4- and 5-periodics (blue). Every trajectory vertex P_i (resp. segment P_iP_{i+1}) is bisected by the local normal $\hat{n}_i$ (resp. tangent to the confocal caustic, brown). A second, equi-perimeter member of each family is also shown (dashed blue). Video

where $\hat{v}$ is the unit incoming (or outgoing) velocity vector, and:

$$\nabla f_i = 2\left(\frac{x_i}{a^2}, \frac{y_i}{b^2}\right).$$

Joachimsthal's constant J can also be expressed in terms of the billiard semiaxes a, b and the major semiaxis a'' of the caustic [23]:

$$J = \frac{\sqrt{a^2 - a''^2}}{ab}.$$

Let κ_i denote the curvature of the elliptic billiard at P_i given by [28, Ellipse]:

$$\kappa = \frac{1}{a^2b^2}\left(\frac{x^2}{a^4} + \frac{y^2}{b^4}\right)^{-3/2}.$$

The signed area of a polygon is given by the following sum of cross-products [17]:

$$A = \frac{1}{2}\sum_{i=1}^{N}(P_{i+1} - P_i) \times (P_i - P_{i+1}).$$

Let $d_{j,i}$ be the distance $|P_i - f_j|$. The inversion $P_{j,i}^\dagger$ of vertex P_i with respect to a circle of radius ρ centered on f_j is given by:

$$P_{j,i}^\dagger = f_j + \left(\frac{\rho}{d_{j,i}}\right)^2(P_i - f_j).$$

The following closed-form expression for k_{119} for all N was contributed by H. Stachel [23]:

$$\sum_{i=1}^{N}\kappa_i^{2/3} = L/[2J(ab)^{4/3}]. \tag{A.1}$$

B. Vertices & caustics $N = 3, 4, 5, 6, 8$

The four intersections of an ellipse with semi-axes a, b with a confocal hyperbola with semi-axes a'', b'' are given by:

B.1. $N = 3$ vertices & caustic

Let $P_i = (x_i, y_i)/q_i$, $i = 1, 2, 3$, denote the 3-periodic vertices, given by [12]:

$$q_1 = 1,$$
$$\begin{aligned}
x_2 &= -b^4\big((a^2 + b^2)k_1 - a^2\big)x_1^3 - 2a^4b^2k_2x_1^2y_1 \\
&\quad + a^4\big((a^2 - 3b^2)k_1 + b^2\big)x_1y_1^2 - 2a^6k_2y_1^3,
\end{aligned}$$
$$\begin{aligned}
y_2 &= 2b^6k_2x_1^3 + b^4\big((b^2 - 3a^2)k_1 + a^2\big)x_1^2y_1 \\
&\quad + 2a^2b^4k_2x_1y_1^2 - a^4\big((a^2 + b^2)k_1 - b^2\big)y_1^3,
\end{aligned}$$
$$q_2 = b^4\big(a^2 - c^2k_1\big)x_1^2 + a^4\big(b^2 + c^2k_1\big)y_1^2 - 2a^2b^2c^2k_2x_1y_1,$$
$$\begin{aligned}
x_3 &= b^4\big(a^2 - (b^2 + a^2)\big)k_1x_1^3 + 2a^4b^2k_2x_1^2y_1 \\
&\quad + a^4\big(k_1(a^2 - 3b^2) + b^2\big)x_1y_1^2 + 2a^6k_2y_1^3,
\end{aligned}$$
$$\begin{aligned}
y_3 &= -2b^6k_2x_1^3 + b^4\big(a^2 + (b^2 - 3a^2)k_1\big)x_1{}^2y_1 \\
&\quad - 2a^2b^4k_2x_1y_1^2 + a^4\big(b^2 - (b^2 + a^2)k_1\big)y_1^3,
\end{aligned}$$
$$q_3 = b^4\big(a^2 - c^2k_1\big)x_1^2 + a^4\big(b^2 + c^2k_1\big)y_1^2 + 2a^2b^2c^2k_2x_1y_1,$$

where:

$$k_1 = \frac{d_1^2\delta_1^2}{d_2} = \cos^2\alpha,$$
$$k_2 = \frac{\delta_1 d_1^2}{d_2}\sqrt{d_2 - d_1^4\delta_1^2} = \sin\alpha\cos\alpha,$$
$$c^2 = a^2 - b^2, \quad d_1 = (ab/c)^2, \quad d_2 = b^4x_1^2 + a^4y_1^2,$$
$$\delta = \sqrt{a^4 + b^4 - a^2b^2}, \quad \delta_1 = \sqrt{2\delta - a^2 - b^2},$$

where α, though not used here, is the angle of segment P_1P_2 (and P_1P_3) with respect to the normal at P_1. The caustic is the ellipse:

$$\frac{x^2}{a''^2} + \frac{y^2}{b''^2} - 1 = 0, \quad a'' = \frac{a(\delta - b^2)}{a^2 - b^2}, \quad b'' = \frac{b(a^2 - \delta)}{a^2 - b^2}.$$

B.2. $N = 4$ vertices & caustic

B.3. Simple

The vertices of the 4-periodic orbit are given by:

$$P_1 = (x_1, y_1), \qquad P_2 = \left(-\frac{a^4y_1}{\sqrt{b^6x_1^2 + a^6y_1^2}}, \frac{b^4x_1}{\sqrt{b^6x_1^2 + a^6y_1^2}}\right),$$

$$P_3 = -P_1, \qquad\qquad P_4 = -P_2.$$

The caustic is the ellipse:

$$\frac{x^2}{a''^2} + \frac{y^2}{b''^2} - 1 = 0, \quad a'' = \frac{a^2}{\sqrt{a^2 + b^2}}, \quad b'' = \frac{b^2}{\sqrt{a^2 + b^2}}.$$

The area and its bounds are given by:

$$A = \frac{2(b^4 x_1^2 + a^4 y_1^2)}{\sqrt{b^6 x_1^2 + a^6 y_1^2}}, \quad \frac{4a^2 b^2}{a^2 + b^2} \le A \le 2ab.$$

The minimum (resp. maximum) area is achieved when the orbit is a rectangle with $P_1 = (x_1, b^2 x_1/a^2)$ (resp. rhombus with $P_1 = (a, 0)$). The perimeter is given by:

$$L = 4\sqrt{a^2 + b^2}. \tag{B.1}$$

Note: when $b = 1$, the perimeter is equal to the $N = 4$ k_{803}.

The exit angle α required to close the trajectory from a departing position (x_1, y_1) on the elliptic billiard boundary is given by:

$$\cos\alpha = \frac{a^2 b}{\sqrt{a^2 + b^2}\sqrt{a^4 - c^2 x_1^2}}.$$

B.3.1. Self-intersected

When $a/b > \sqrt{2}$, the vertices of the 4-periodic self-intersecting orbit are given by:

$$P_1 = \left[au, b\sqrt{1 - u^2}\right], \quad P_3 = \left[-au, b\sqrt{1 - u^2}\right],$$

$$P_2 = \left[-\frac{a\sqrt{a^2(a^2 - 2b^2) - c^4 u^2}}{c^2\sqrt{1 - u^2}}, -\frac{b^3}{c^2\sqrt{1 - u^2}}\right],$$

$$P_4 = \left[\frac{a\sqrt{a^2(a^2 - 2b^2) - c^4 u^2}}{c^2\sqrt{1 - u^2}}, -\frac{b^3}{c^2\sqrt{1 - u^2}}\right],$$

where $|u| \le \frac{a}{c^2}\sqrt{a^2 - 2b^2}$. The confocal hyperbolic caustic is given by:

$$\frac{x^2}{a''^2} - \frac{y^2}{b''^2} = 1, \quad a'' = \frac{a\sqrt{a^2 - 2b^2}}{c}, \quad b'' = \frac{b^2}{c}.$$

The four intersections of an ellipse with semi-axes a, b with confocal hyperbola with axes a'', b'' are given by:

$$\left[\pm\frac{aa''}{c}, \pm\frac{bb''}{c}\right]. \tag{B.2}$$

The exit angle α required to close the trajectory from a departing position (x_1, y_1) on the elliptic billiard boundary is given by:

$$\cos \alpha = \frac{a^2 b}{c\sqrt{a^4 - c^2 x_1^2}}.$$

The perimeter of the orbit is $L = 4a^2/c$.

B.4. $N = 5$ vertices & caustic

Let $a > b$ be the semi-axes of the elliptic billiard.

Proposition B.1. *The major semiaxis length a'' of the caustic for $N = 5$ simple (resp. self-intersecting, i.e., pentagram) is given by the root of the largest (resp. smallest) real root $x \in (0, a)$ of the following bi-sextic polynomial:*

$$\begin{aligned}
P_5(x) = {} & c^{12} x^{12} - 2c^4 a^2 \big(3a^8 - 9a^6 b^2 + 31a^4 b^4 + a^2 b^6 + 6b^8\big) x^{10} \\
& + c^4 a^4 \big(15a^8 - 30a^6 b^2 + 191a^4 b^4 + 16a^2 b^6 + 16b^8\big) x^8 \\
& - 4c^4 a^{10} \big(5a^4 - 5a^2 b^2 + 66b^4\big) x^6 \\
& + a^{12} \big(15a^8 - 30a^6 b^2 + 191a^4 b^4 - 368a^2 b^6 + 208b^8\big) x^4 \\
& - 2a^{14} \big(3a^8 - 3a^6 b^2 + 22a^4 b^4 - 48a^2 b^6 + 32b^8\big) x^2 + a^{24}.
\end{aligned}$$

Proof. Consider a 5-periodic with vertices P_i, $i = 1, \ldots, 5$ where P_1 is at $(a, 0)$, i.e., the orbit is "horizontal". The polynomial P_5 is exactly the Cayley condition for the existence of 5-periodic orbits, see [11]. For $c = 0$ the roots are $a_2' = (\sqrt{5} - 1)a/4$ and $a_2'' = (\sqrt{5} + 1)a/4$ and corresponds to the regular case. For $b = 0$ the roots are coincident in given by $x = a$. By analytic continuation, for $c \in (0, a)$, the two roots are in the interval $(0, a)$. $\qquad \square$

For $N = 5$ non-intersecting, the abcissae of vertices $P_2 = (x_2, y_2)$, $P_3 = (x_3, y_3)$ are given by the smallest positive solution (resp. unique negative) of the following equations:

$$\begin{aligned}
x_2 : {} & c^6 x_2^6 - 2a\big(2a^2 - b^2\big)c^4 x_2^5 + a^2\big(5a^2 + 4b^2\big)c^4 x_2^4 - 8a^5 b^2 c^2 x_2^3 \\
& - a^8\big(5a^2 - 9b^2\big) x_2^2 + 2a^9\big(2a^2 - b^2\big) x_2 - a^{12} = 0, \\
x_3 : {} & c^6 x_3^6 - 2ab^2 c^2\big(3a^2 + b^2\big) x_3^5 - a^2 c^2\big(3a^4 - 3a^2 b^2 + 4b^4\big) x_3^4 + 12a^5 b^2 c^2 x_3^3 \\
& + a^6\big(3a^4 - 3a^2 b^2 + 4b^4\big) x_3^2 - 2a^7 b^2\big(3a^2 - 4b^2\big) x_3 - a^{12} = 0.
\end{aligned}$$

Joachimsthal's constant J for the simple orbit is the smallest positive root of:

$$\begin{aligned}
& 4096 c^{12} J^{12} + 2048(3a^2 + b^2)(a^2 + 3b^2)(a^2 + b^2) c^4 J^{10} \\
& - 256(29a^4 + 54a^2 b^2 + 29b^4) c^4 J^8 + 2304(a^2 + b^2) c^4 J^6 \\
& - 16(3a^2 - 4ab - 3b^2)(3a^2 + 4ab - 3b^2) J^4 - 40(a^2 + b^2) J^2 + 5 = 0.
\end{aligned}$$

The perimeter of the simple orbit is given by $L = p/q$ where:

$$p = \left(1024\left(a^2 + b^2\right)c^4b^2J^7 - 256c^4b^2J^5 - 64\left(a^2 + b^2\right)b^2J^3 + 16Jb^2\right)\sqrt{1 - 4a^2J^2}$$
$$- 1024c^2\left(5a^4 + 2a^2b^2 + b^4\right)b^2J^7 + 256c^2\left(3a^2 + b^2\right)b^2J^5 + 64c^2b^2J^3 + 16Jb^2$$
$$q = 256c^8J^8 - 256c^2\left(a^2 + b^2\right)^2J^6 + 32c^2\left(3a^2 + 5b^2\right)J^4 - 16c^2J^2 + 1.$$

B.5. $N = 6$ vertices & caustic

B.5.1. Simple

Vertices $P_i, i = 2, ..., 6$ with $P_1 = (a, 0)$ are given by:

$$P_4 = [-a, 0], \quad P_2 = [k_x, k_y], \quad P_5 = -P_2, \quad P_3 = [-k_x, k_y], \quad P_6 = -P_3,$$
$$k_x = \frac{a^2}{a + b}, \quad k_y = \frac{b\sqrt{b(2a + b)}}{a + b}.$$

The confocal, elliptic caustic is given by:

$$\frac{x^2}{a''^2} + \frac{y^2}{b''^2} = 1, \quad a'' = \frac{a\sqrt{a(a + 2b)}}{a + b}, \quad b'' = \frac{b\sqrt{b(2a + b)}}{a + b}.$$

The perimeter is given by:

$$L = \frac{4(a^2 + ab + b^2)}{a + b}.$$

B.5.2. Self-Intersected (type I)

This orbit only exists for $a > 2b$. Vertices P_i, $i = 2, \ldots, 6$ with $P_1 = (0, b)$ are given by:

$$P_4 = [0, -b], \quad P_2 = [k_x, k_y], \quad P_5 = -P_2, \quad P_3 = [k_x, -k_y], \quad P_6 = -P_3,$$
$$k_x = \frac{a\sqrt{a(a - 2b)}}{b - a}, \quad k_y = \frac{b^2}{b - a}.$$

The confocal, hyperbolic caustic is given by:

$$\frac{x^2}{a''^2} - \frac{y^2}{b''^2} = 1, \quad a'' = \frac{a^{3/2}\sqrt{a - 2b}}{a - b}, \quad b'' = \frac{b^{3/2}\sqrt{2a - b}}{a - b}.$$

The 4 intersections of the above caustic with the elliptic billiard are given by (B.2). The perimeter is given by:

$$L = \frac{4(a^2 - ab + b^2)}{a - b}.$$

B.5.3. Self-intersected (type II)

This orbit only exists for $a > \frac{2b\sqrt{3}}{3}$. Vertices P_i, $i = 2, \ldots, 6$ with $P_1 = [0, b]$ are given by:

$$P_4 = [0, -b], \quad P_2 = [k_x, k_y], \quad P_3 = -P_2, \quad P_5 = [k_x, -k_y], \quad P_6 = -P_5$$

$$k_x = -\frac{a^{\frac{3}{2}}\sqrt{2c - a}}{c}, \quad k_y = \frac{(c - a)b}{c}.$$

The confocal hyperbolic caustic is given by:

$$\frac{x^2}{a''^2} - \frac{y^2}{b''^2} = 1, \quad a''^2 = \frac{a^3\left(3ac - 2b^2\right)}{c(3a^2 + b^2)}, \quad b''^2 = \frac{b^2\left(2a^2(a - c) - b^2c\right)}{c(3a^2 + b^2)}.$$

The 4 intersections of the above caustic with the elliptic billiard are given by (B.2). The perimeter is given by:

$$L = 4(a + c)\sqrt{2a/c - 1}.$$

B.6. $N = 7$ caustic

Referring to Figure 1, there are three types of 7-periodics: (i) non-intersecting, (ii) self-intersecting type I, i.e., with turning number 2, (iii) self-intersecting type II.

Proposition B.2. *The caustic semiaxis for non-intersecting 7-periodics (resp. self-intersecting type I, and type II self-intersecting) are given by the smallest (resp. second and third smallest) root of the following degree-12 polynomial:*

$$c^{12}x_1^{12} - 4\left(a^2 + b^2\right)c^6a\left(3a^2 + b^2\right)b^2x_1^{11} - 2c^6a^2\left(3a^6 - 6a^4b^2 + 13a^2b^4 - 2b^6\right)x_1^{10}$$
$$+ c^6a^3\left(60a^4 + 60b^2a^2 + 8b^4\right)x_1^9$$
$$+ a^6c^2\left(15a^8 - 45a^6b^2 + 125a^4b^4 - 143a^2b^6 + 112b^8\right)x_1^8$$
$$- 8a^7b^2c^2\left(15a^6 - 20a^4b^2 - 7a^2b^4 + 8b^6\right)x_1^7$$
$$- 4a^8c^2\left(5a^8 - 10a^6b^2 + 35a^4b^4 - 30a^2b^6 + 36b^8\right)x_1^6$$
$$+ 8a^9b^2c^2\left(15a^6 - 25a^4b^2 - 2a^2b^4 + 4b^6\right)x_1^5$$
$$+ a^{10}c^2\left(15a^8 - 15a^6b^2 + 80a^4b^4 - 32a^2b^6 + 64b^8\right)x_1^4$$
$$- 4a^{15}b^2\left(15a^4 - 45b^2a^2 + 32b^4\right)x_1^3$$
$$- 2a^{16}\left(3a^6 - 3a^4b^2 + 10a^2b^4 - 8b^6\right)x_1^2 + 4a^{17}b^2\left(3a^2 - 4b^2\right)\left(a^2 - 2b^2\right)x_1 + a^{24}$$
$$= 0.$$

It can shown the first two smallest (resp. third smallest) roots of the above polynomial are negative (resp. positive), and all have absolute values within $(0, a)$.

For $a = b$ the polynomial equation above is given by $a^3 + 4a^2x_1 - 4ax_12 - 8x_1^3 = 0$ with roots $-0.9009688680a$, $-0.2225209340a$, $0.6234898025a$.

B.7. $N = 8$ vertices & caustic

B.7.1. Simple

Let P_i, $i = 1, \ldots, 8$ be the vertices of a simple 8-periodic, Figure 10. Set $P_1 = [a, 0]$. Then:

$$P_5 = -[a, 0], \quad P_3 = [0, b], \quad P_7 = [0, -b], \quad P_{2,4,6,8} = [\pm az, \pm b\sqrt{1 - z^2}],$$

where z, which plays the role of a cosine, is the only positive root of $c^4 z^4 - 2a^2 c^2 z^3 + 2a^2 b^2 z^2 + 2a^2 c^2 z - a^4 = 0$.

Remark B.3. Given an ellipse with semi-axes (a, b), let $P_1 = [a, 0]$ and $P_2 = [a \cos t, b \sin t]$. Let $z = \cos t$. The unique confocal ellipse which is tangent to the chord $P_1 P_2$ has major axis a'' given by:

$$a'' = a\sqrt{\frac{a^2 - z(a^2 - 2b^2)}{a^2 + b^2 - zc^2}}.$$

Recall confocality implies $b'' = \sqrt{a''^2 - c^2}$. Therefore, one can use the above to compute from z the semi-axes of the caustic for simple 8-periodics.

B.7.2. Self-intersected (type I and type II)

These have hyperbolic confocal caustics; see Figures 11 and 12. Let $P_1 = (x_1, y_1)$ be at the intersection of the hyperbolic caustic with the elliptic billiard for each case. For type-I (resp. type-II) x_1 is given by the smallest (resp. largest) positive root $x_1 \in (0, a)$ of the following degree-8 polynomial:

$$\begin{aligned} x_1 : \ & c^{16} x_1^8 - 4a^4 c^8 \big(a^6 - 4a^4 b^2 + a^2 b^4 - 2b^6\big) x_1^6 + 2a^8 c^6 \big(3a^6 - 15a^4 b^2 - 4b^6\big) x_1^4 \\ & - 4a^{16} c^4 \big(a^2 - 6b^2\big) x_1^2 + a^{20} \big(a^4 - 8a^2 b^2 + 8b^4\big) = 0. \end{aligned}$$

From (B.2) obtain the major semi-axis for confocal caustic: $a'' = (x_1 c)/a$, and $b'' = \sqrt{c^2 - a''^2}$.

B.7.3. Self-intersected (type III)

The confocal caustic is an ellipse with semi-axes (a'', b''). Let $P_1 = (a'', y_1)$ and $P_2 = (a'', -y_1)$ be two consecutive vertices in the doubled-up type III 8-periodic (dashed red in Figure 13) connected by a vertical line (the figure is rotated, therefore this line will appear horizontal). Let $\alpha = a/b$. The square of a'' is given by the smallest positive root of the following quartic polynomial:

$$\begin{aligned} & \alpha^{16} + \big(\alpha^2 - 1\big)^2 \big(\alpha^4 + 6\alpha^2 + 1\big) x^4 - 4\big(\alpha^2 - 1\big)^2 \big(\alpha^2 + 5\big)\alpha^4 x^3 + \\ & \big(6\big(\alpha^4 + 2\alpha^2 - 7\big)\alpha^2 + 32\big)\alpha^6 x^2 - 4\big(\alpha^6 + \alpha^4 - 4\alpha^2 + 4\big)\alpha^8 x = 0. \end{aligned}$$

Note: $b'' = \sqrt{a''^2 - c^2}$.

C. Table of symbols

Table 3. Symbols used in the invariants.
Note $i \in [1, N]$ and $j = 1, 2$.

symbol	meaning
O, N	center of elliptic billiard and vertex count
L, J	inv. perimeter and Joachimsthal's constant
a, b	elliptic billiard major, minor semi-axes
a'', b''	caustic major, minor semi-axes
f_1, f_2	foci
P_i, P_i', P_i''	N-periodic, outer, inner polygon vertices
$d_{j,i}$	distance $|P_i - f_j|$
κ_i	ellipse curvature at P_i
θ_i, θ_i'	N-periodic, outer polygon angles
A, A', A''	N-periodic, outer, inner areas
ρ	radius of the inversion circle
$P_{j,i}^{\dagger}$	vertices of the inversive polygon wrt f_j
$L_j^{\dagger}, A_j^{\dagger}$	perimeter, area of inversive polygon wrt f_j
$\theta_{j,i}^{\dagger}$	ith angle of inversive polygon wrt f_j

References

[1] A. AKOPYAN: *Corollary of Theorem 6 in Akopyan et al., "Billiards in Ellipses Revisited" (2020)*. Private Communication, Jan. 2020.

[2] A. AKOPYAN, R. SCHWARTZ, S. TABACHNIKOV: *Billiards in Ellipses Revisited*, Eur. J. Math. (Sept. 2020), DOI: https://doi.org/10.1007/s40879-020-00426-9.

[3] D. BARALIĆ, I. SPASOJEVIĆ: *Illumination of Pascal's Hexagrammum and Octagrammum Mysticum*, Discrete & Computational Geometry 53.2 (2015).

[4] M. V. BERRY: *Regularity and chaos in classical mechanics, illustrated by three deformations of a circular 'billiard'*, Eur. J. Phys. 2.91 (1981).

[5] M. BIALY, S. TABACHNIKOV: *Dan Reznik's Identities and More*, Eur. J. Math. (Sept. 2020), DOI: https://doi.org/10.1007/s40879-020-00428-7.

[6] G. BIRKHOFF: *On the periodic motions of dynamical systems*, Acta Mathematica 50.1 (1927), pp. 359–379, DOI: https://doi.org/10.1007/BF02421325.

[7] G. D. BIRKHOFF: *Dynamical Systems*, 1966th ed., vol. 9, Colloqium Publications, Providence, RI: American Mathematical Society, 1927.

[8] A. CHAVEZ-CALIZ: *More About Areas and Centers of Poncelet Polygons*, Arnold Math J. (Aug. 2020), DOI: https://doi.org/10.1007/s40598-020-00154-8.

[9] A. CONNES, D. ZAGIER: *A Property of Parallelograms Inscribed in Ellipses*, The American Mathematical Monthly 114.10 (2007), pp. 909–914.

[10] D. R. DA COSTA, C. P. DETTMANN, E. D. LEONEL: *Circular, elliptic and oval billiards in a gravitational field*, Comm. in Nonlin. Sci. and Num. Sim. 22.1 (2015), pp. 731–746.

[11] V. DRAGOVIĆ, M. RADNOVIĆ: *Poncelet Porisms and Beyond: Integrable Billiards, Hyperelliptic Jacobians and Pencils of Quadrics*, Frontiers in Mathematics, Basel: Springer, 2011.

[12] R. GARCIA: *Elliptic Billiards and Ellipses Associated to the 3-Periodic Orbits*, American Mathematical Monthly 126.06 (2019), pp. 491–504, DOI: https://doi.org/10.1080/000298 90.2019.1593087.

[13] R. GARCIA, D. REZNIK, J. KOILLER: *New Properties of Triangular Orbits in Elliptic Billiards*, Amer. Math. Monthly (Oct. 2021), DOI: https://doi.org/10.1080/00029890.2021.1982360.

[14] R. A. JOHNSON: *Modern Geometry: An Elementary Treatise on the Geometry of the Triangle and the Circle*, Boston, MA: Houghton Mifflin, 1929.

[15] V. KALOSHIN, A. SORRENTINO: *On the Integrability of Birkhoff Billiards*, Phil. Trans. R. Soc. A.376 (2018), DOI: https://doi.org/10.1098/rsta.2017.0419.

[16] M. LEVI, S. TABACHNIKOV: *The Poncelet Grid and Billiards in Ellipses*, The American Mathematical Monthly 114.10 (2007), pp. 895–908, DOI: https://doi.org/10.1080/000298 90.2007.11920482.

[17] F. PREPARATA, M. SHAMOS: *Computational Geometry - An Introduction*, 2nd, Basel: Springer-Verlag, 1988.

[18] R. RAMÍREZ-ROS: *On Cayley conditions for billiards inside ellipsoids*, Nonlinearity 27.5 (2014), pp. 1003–1028, DOI: https://doi.org/10.1088/0951-7715/27/5/1003.

[19] D. REZNIK, R. GARCIA, J. KOILLER: *Can the Elliptic Billiard still surprise us?*, Math Intelligencer 42 (2020), pp. 6–17, DOI: https://doi.org/10.1007/s00283-019-09951-2.

[20] D. REZNIK, R. GARCIA, J. KOILLER: *Eighty New Invariants of N-Periodics in the Elliptic Billiard*, arXiv:2004.12497, Nov. 2020.

[21] D. REZNIK, R. GARCIA, J. KOILLER: *Fifty New Invariants of N-Periodics in the Elliptic Billiard*, Arnold Math. J. 7 (2021), pp. 341–355, DOI: https://doi.org/10.1007/s40598-02 1-00174-y.

[22] R. SCHWARTZ: *The Poncelet grid*, Advances in Geometry 7.2 (2007), pp. 157–175, DOI: http s://doi.org/10.1515/ADVGEOM.2007.010.

[23] H. STACHEL, Private Communication, 2020.

[24] H. STACHEL: *On the motion of billiards in ellipses*, Eur. J. of Math. (2021), DOI: https://d oi.org/10.1007/s40879-021-00524-2.

[25] H. STACHEL: *The geometry of billiards in ellipses and their Poncelet grids*, Journal of Geometry 112.40 (2021).

[26] S. TABACHNIKOV: *Geometry and Billiards*, vol. 30, Student Mathematical Library, Providence, RI: American Mathematical Society, 2005.

[27] VARIOUS CONTRIBUTORS: *Antiparallelogram*, Wikipedia, 2021, URL: https://en.wikipedia .org/wiki/Antiparallelogram.

[28] E. W. WEISSTEIN: *CRC concise encyclopedia of mathematics (2nd ed.)* Boca Raton, FL: Chapman and Hall/CRC, 2002.